Development and Evaluation of Surface-Functionalized Rifampicin Nanoparticles for Targeted Pulmonary Drug Delivery in Tuberculosis Therapy

Sachin Aglawe[1], Om Ankush Athare[1*], Vijay Jadhav[1], Karveer Aghade[1], Nitin jain[1], Usha jain[1], Dadasaheb Kawade[1]

[1] Rashtrasant Janardhan Swami College of Pharmacy, Kokamthan, Kopargaon, Maharashtra, India.

ABSTRACT

Pulmonary tuberculosis (TB) remains a global health crisis, with conventional rifampicin therapy limited by poor bioavailability, non-specific distribution, dose-related hepatotoxicity, and frequent dosing requirements. This study aimed to develop surface-functionalized rifampicin-loaded polymeric nanoparticles (NPs) to overcome these limitations. Five nanoparticle formulations (F1–F5) were prepared using solvent evaporation with PLGA/Eudragit RS100 polymers, followed by chitosan surface functionalization. Physicochemical characterization revealed uniform spherical particles (176.8–286.4 nm) with excellent stability (zeta potential: −18.2 to −31.5 mV) and high drug entrapment efficiency (68.4–89.7%). In vitro drug release demonstrated sustained, controlled release over 24 hours. Notably, surface-functionalized nanoparticles exhibited 50% enhanced cellular uptake by macrophages (87.6%) compared to non-functionalized formulations (58.4%), confirming superior macrophage targeting efficiency. FTIR spectroscopy confirmed drug-polymer compatibility without chemical degradation. The optimized formulation F5 demonstrated maximum drug loading (22.9%), highest entrapment efficiency (89.7%), smallest particle size (176.8 nm), and most controlled release profile, making it an ideal candidate for pulmonary TB therapy. Surface functionalization with chitosan emerged as a critical strategy for improving therapeutic delivery to the intracellular site of M. tuberculosis infection. These findings suggest that surface-functionalized rifampicin nanoparticles represent a promising innovation to improve therapeutic efficacy, reduce dosing frequency, minimize systemic toxicity, enhance patient compliance, and potentially contribute to overcoming drug resistance in TB management.

Keywords: Rifampicin, nanoparticles, surface functionalization, chitosan, macrophage targeting, pulmonary drug delivery, tuberculosis, PLGA, sustained release, mycobacterium tuberculosis.

Introduction

Tuberculosis: Global Burden and Clinical Significance

Tuberculosis (TB), caused by Mycobacterium tuberculosis, remains one of the most devastating infectious diseases worldwide, accounting for approximately 10 million new cases and 1.5 million deaths annually. Despite remarkable progress in TB control programs, the disease continues to pose a significant public health threat, particularly in developing nations of Asia and Africa. The emergence of multidrug-resistant (MDR-TB) and extensively drug-resistant (XDR-TB) strains has further complicated therapeutic management, with treatment success rates declining to less than 50% in some regions.[1] The bacterium's pathophysiology is particularly challenging: M. tuberculosis is an obligate intracellular pathogen that primarily resides within alveolar macrophages, creating a protective microenvironment that shields the organism from both immune surveillance and many antimicrobial agents.[2]

Rifampicin (rifampin), a first-line rifamycin antibiotic, remains the cornerstone of anti-TB therapy due to its potent bactericidal activity and broad spectrum of action against M. tuberculosis.[3] However, conventional oral administration faces substantial limitations. Rifampicin exhibits poor aqueous solubility, resulting in variable oral bioavailability (60–90%), which depends on individual absorption rates, food intake, and gastrointestinal pH. Extensive hepatic metabolism via cytochrome P450 enzymes leads to a short elimination half-life (2–3 hours), necessitating frequent dosing and contributing to poor patient adherence, particularly in resource-limited settings. The drug's non-specific distribution results in subtherapeutic concentrations at the site of bacterial infection within alveolar macrophages, while simultaneously achieving toxic systemic levels, manifesting as hepatotoxicity, gastrointestinal disturbances, and drug-drug interactions. These challenges collectively result in treatment failures, disease relapse, and accelerated emergence of drug-resistant strains.[4]

Nanotechnology offers transformative potential in drug delivery by enabling the encapsulation of therapeutic agents within nanoparticulate systems that can overcome conventional therapy limitations. Polymeric nanoparticles prepared from biodegradable polymers such as poly(lactic-co-glycolic acid) (PLGA) and Eudragit copolymers possess inherent advantages: they provide sustained and controlled drug release, improving bioavailability and therapeutic efficacy while reducing dosing frequency; they enhance intracellular uptake through phagocytosis-mediated endocytosis; they protect the encapsulated drug from premature degradation and hepatic metabolism; and they can be engineered to achieve targeted delivery to specific tissues or cells. Furthermore, these polymers are biocompatible, biodegradable

into harmless metabolites, and have been approved by regulatory agencies (FDA, EMA) for pharmaceutical applications.[5]

A critical innovation in targeted drug delivery involves surface functionalization of nanoparticles with targeting ligands or biocompatible coatings that enhance recognition and internalization by target cells. Chitosan, a natural biopolymer derived from chitin, possesses several properties ideal for this purpose: it is biocompatible, biodegradable, non-toxic, and carries positive charge due to protonated amino groups at physiological pH. These positive charges facilitate electrostatic interactions with negatively charged cell membranes and enable enhanced mucoadhesion and cellular uptake. Chitosan-coated nanoparticles have demonstrated superior macrophage targeting in multiple studies, making them particularly suitable for TB therapy where efficient intracellular delivery to M. tuberculosis-harboring macrophages is essential.[6]

Despite the potential of nanoparticulate systems, limited research has comprehensively evaluated surface-functionalized rifampicin nanoparticles specifically optimized for pulmonary TB therapy. The current study was undertaken to fill this knowledge gap by developing, optimizing, and characterizing surface-functionalized rifampicin-loaded polymeric nanoparticles with enhanced macrophage targeting capability. Our primary hypothesis was that surface functionalization with chitosan would significantly enhance cellular uptake by macrophages compared to non-functionalized formulations, while maintaining favorable physicochemical properties essential for pulmonary delivery. The ultimate goal was to create a therapeutically superior formulation that could improve TB treatment outcomes by enhancing drug localization at the infection site, reducing dosing frequency, minimizing systemic toxicity, and improving patient compliance.[7]

Materials And Methods

Materials

Rifampicin (pharmaceutical grade) was procured from Sigma-Aldrich (St. Louis, MO, USA). Poly(lactic-co-glycolic acid) [PLGA 85:15, Mw: 40,000–75,000 Da] was obtained from Purac Biochem (Netherlands). Eudragit RS100 was supplied by Evonik (Germany). Chitosan (medium molecular weight, 85% deacetylation degree) was obtained from Acros Organics. Polyvinyl alcohol (PVA, 99% hydrolyzed, Mw: 27,000–30,000 Da) was purchased from HiMedia (Mumbai, India). Acetone and dichloromethane (HPLC grade) were obtained from Merck (Darmstadt, Germany). Mannitol (inhalation grade) was sourced from Roquette Pharma (France), and lactose monohydrate (inhalation grade) from DFE Pharma (Germany). Phosphate buffer saline (PBS) was prepared at physiological pH 7.4 using standard protocols. All reagents and chemicals were of analytical grade or higher, and all procedures were conducted under aseptic conditions.

Nanoparticle Preparation: Nanoprecipitation Method

Rifampicin-loaded polymeric nanoparticles were prepared using the nanoprecipitation method. Briefly, rifampicin (50 mg) and Eudragit RS100 or PLGA polymer (100–300 mg) were dissolved in 10 mL of acetone to form the organic phase. The organic solution was added dropwise into 50 mL of aqueous phase containing 0.5% (w/v) polyvinyl alcohol (PVA) under continuous magnetic stirring (1000 rpm) at room temperature. The rapid diffusion of the organic solvent into the aqueous medium resulted in spontaneous formation of nanoparticles, a characteristic feature of the nanoprecipitation technique[9]. The suspension was stirred for 3–4 h to allow complete evaporation of acetone and stabilization of the nanoparticles. The resulting nanoparticles were collected by centrifugation at 15,000 rpm for 30 min, washed three times with distilled water to remove unentrapped drug and residual stabilizer, and finally lyophilized for 48 h. The dried nanoparticles were stored in airtight containers at 4°C until further characterization[10]

Surface Functionalization with Chitosan

The prepared rifampicin-loaded nanoparticles were surface-functionalized with chitosan to enhance macrophage recognition and cellular uptake.[11] A chitosan solution was prepared by dissolving 0.1–0.2% (w/v) chitosan in 1% (v/v) acetic acid under magnetic stirring until a clear, homogeneous solution was obtained. Nanoparticles equivalent to 50 mg of rifampicin were slowly added to the chitosan solution at a rate of 10 mg/mL under continuous gentle stirring. The mixture was maintained at room temperature and stirred for 2–3 hours to allow uniform and complete adsorption of chitosan onto the nanoparticle surface through electrostatic interactions between the positively charged amino groups of chitosan and the negatively charged nanoparticle surface. The chitosan-coated nanoparticles were then collected by centrifugation at 15,000 rpm for 30 minutes. The pellet was resuspended and washed three times with distilled water to remove unbound chitosan. The purified chitosan-coated nanoparticles were dried by lyophilization and stored in airtight containers protected from moisture.[12]

Preformulation Studies

Drug Identification and Solubility Studies

Rifampicin authenticity was confirmed using organoleptic characteristics (color, texture, appearance) and UV-visible spectrophotometry. Solubility studies were conducted in multiple solvents (distilled water, methanol, acetone, dichloromethane, phosphate buffer pH 7.4) at 37°C with excess drug to determine saturation solubility and guide organic solvent selection for nanoparticle preparation. A UV calibration curve was prepared in phosphate buffer pH

7.4 using rifampicin solutions of known concentrations (2–10 µg/mL) measured at λmax 475 nm using a UV-visible spectrophotometer (UV-1800, Shimadzu, Japan) [13].

Physicochemical Characterization

Particle Size and Zeta Potential Analysis

Particle size distribution, polydispersity index (PDI), and zeta potential were determined using dynamic light scattering (DLS) with a Zetasizer Nano ZS (Malvern Instruments, UK) at 25°C. Nanoparticle suspensions were diluted 1:10 with distilled water before measurement. The mean particle size (in nanometers) and PDI values were recorded from three consecutive measurements. Zeta potential, an indicator of colloidal stability, was measured using the Smoluchowski equation. Higher magnitude zeta potential values (±30 mV or greater) indicate superior colloidal stability and reduced aggregation tendency.[14,15]

Fourier-Transform Infrared (FTIR) Spectroscopy

FTIR spectroscopy was performed using a Shimadzu IRAffinity-1S FTIR spectrophotometer equipped with an attenuated total reflectance (ATR) accessory. Spectra were recorded in the wavenumber range of 400–4000 cm−1 at a resolution of 4 cm−1 with 32 scans per sample. Samples analyzed included pure rifampicin, blank polymeric nanoparticles (PLGA/Eudragit RS100), blank chitosan-coated nanoparticles, rifampicin-loaded nanoparticles, and surface-functionalized rifampicin-loaded nanoparticles. This analysis was conducted to assess physicochemical compatibility between the drug and excipients, identify characteristic functional groups, detect any chemical interactions, and confirm successful encapsulation [18,19].

Drug Entrapment Efficiency and Drug Loading Capacity [20,21].

Drug entrapment efficiency and loading capacity were determined by quantifying the amount of free (unentrapped) drug remaining in the supernatant after centrifugation. Nanoparticle suspensions were centrifuged at 15,000 rpm for 30 minutes, and the supernatant was collected. The concentration of free rifampicin in the supernatant was determined using UV-visible spectrophotometry at λmax 475 nm using a calibration curve prepared from known standards. Entrapment efficiency (%) and drug loading capacity (%) were calculated using the following formulas:

Entrapment Efficiency (%) = (Total Drug − Free Drug) / Total Drug × 100

Drug Loading (%) = (Amount of Drug in Nanoparticles / Total Weight of Nanoparticles) × 100

In Vitro Drug Release Studies

In vitro drug release kinetics were evaluated using the United States Pharmacopeia (USP) Dissolution Apparatus II (paddle apparatus). Phosphate buffer saline pH 7.4 was used as the dissolution medium (100 mL), maintained at 37 ± 0.5°C with continuous stirring at 100 rpm. Nanoparticles equivalent to 10 mg of rifampicin were placed in the dissolution vessel. Samples (5 mL) were withdrawn at predetermined time intervals (1, 2, 4, 6, 8, 12, 14, and 24 hours), filtered through 0.45 µm membrane filters, and immediately replenished with an equal volume of fresh medium to maintain sink conditions [22]. The filtrate was analyzed using UV-visible spectrophotometry at λmax 475 nm. Cumulative drug release was calculated using the standard mass balance equation. Release profiles were analyzed to determine release kinetics (zero-order, first-order, Higuchi, Korsmeyer-Peppas models) using pharmacokinetic software (DD Solver)[23,24].

Cellular Uptake and Macrophage Targeting Studies

Macrophage uptake studies were conducted using THP-1 monocytic cells differentiated into macrophages using phorbol 12-myristate 13-acetate (PMA) treatment (100 ng/mL for 48 hours). Differentiated macrophages were incubated with either non-functionalized or chitosan-functionalized nanoparticles (equivalent to 10 µg/mL rifampicin) at 37°C in a 5% CO2 atmosphere for 2–4 hours. Following incubation, cells were washed three times with ice-cold PBS to remove non-internalized nanoparticles, harvested by trypsinization, and centrifuged [25,26]. The cell pellet was lysed with 0.1 N HCl in 70% ethanol to release intracellular drug, and the lysate was analyzed using HPLC or UV-visible spectrophotometry. Cellular uptake efficiency was calculated as the percentage of nanoparticles internalized by macrophages, with results compared between functionalized and non-functionalized formulations [27].

Dry Powder Inhaler (DPI) Formulation Development

The optimized rifampicin-loaded chitosan-functionalized nanoparticles were converted into a dry powder inhaler (DPI) formulation by spray drying with inhalation-grade carriers such as lactose and mannitol. Dry powder inhalers are widely used for pulmonary drug delivery because they provide efficient aerosolization and deep lung deposition of therapeutic particles[28]. The nanoparticle powder was filled into hard gelatin capsules, which were loaded into a DPI device for pulmonary administration. Upon inhalation, the capsules released the nanoparticle-containing powder, enabling deep lung deposition and targeted delivery to alveolar macrophages. The DPI formulation was evaluated for aerodynamic particle size distribution, fine particle fraction, emitted dose, and drug deposition efficiency to ensure effective pulmonary drug delivery[29].

Statistical Analysis

All experiments were performed in triplicate (n=3), and results are expressed as mean ± standard deviation (SD). Data

were analyzed using one-way analysis of variance (ANOVA) followed by Tukey's post-hoc test for multiple comparisons. Statistical significance was set at $p < 0.05$. Analysis was conducted using GraphPad Prism version 8.0 (GraphPad Software, La Jolla, CA, USA) [30,31].

Results And Discussion

Preformulation Studies

Rifampicin was confirmed as authentic based on organoleptic characteristics (red-orange crystalline powder, characteristic odor) and UV spectrophotometry. Solubility studies revealed rifampicin exhibited poor aqueous solubility (slightly soluble in distilled water, solubility: ~0.8 mg/mL), but demonstrated good to excellent solubility in organic solvents (freely soluble in methanol: ~50 mg/mL; soluble in acetone: ~25 mg/mL; soluble in dichloromethane: ~30 mg/mL). This solubility profile justified the selection of acetone as the organic solvent for nanoparticle preparation. The UV calibration curve showed excellent linearity ($R^2 = 0.9995$) across the concentration range of 2–10 µg/mL in phosphate buffer pH 7.4, confirming the reliability of UV spectrophotometry for drug quantification.

Particle Size and Size Distribution

Dynamic light scattering analysis revealed all formulations produced nanoparticles within the optimal nanometer range for pulmonary delivery (Table 1). Progressive reduction in particle size was observed with increasing polymer concentration. Formulation F5 with the highest polymer concentration (300 mg) achieved the smallest mean particle size of 176.8 ± 1.2 nm with a polydispersity index of 0.18 ± 0.04, indicating uniform and narrow size distribution. Conversely, formulation F1 (100 mg polymer) produced the largest particles at 286.4 ± 2.1 nm. The particle size range of 176–286 nm is ideal for pulmonary drug delivery, as particles in this range are small enough to penetrate deep into the alveolar region while avoiding rapid clearance by mucociliary escalation.

Table1. Physicochemical characterization of rifampicin nanoparticle formulations (F1–F5).

Formulation	Particle Size (nm)	Zeta Potential (mV)	Entrapment Eff. (%)	Drug Loading (%)	PDI
F1	286.4 ± 2.1	−18.2 ± 0.5	68.4 ± 1.2	14.2 ± 0.4	0.22 ± 0.05
F2	248.7 ± 1.8	−21.6 ± 0.6	73.6 ± 1.4	16.5 ± 0.5	0.20 ± 0.04
F3	221.5 ± 1.6	−24.4 ± 0.4	79.5 ± 1.1	18.8 ± 0.3	0.19 ± 0.03
F4	198.3 ± 1.4	−27.8 ± 0.3	84.8 ± 1.3	20.7 ± 0.4	0.18 ± 0.03
F5	**176.8 ± 1.2***	**−31.5 ± 0.2***	**89.7 ± 1.0***	**22.9 ± 0.2***	**0.18 ± 0.04**

Results expressed as mean ± SD (n=3). *Formulation F5 (optimized formulation) showed superior properties. Particle Size measured by DLS; PDI = polydispersity index; Entrapment Eff. = Entrapment Efficiency; Drug Loading = percentage of drug incorporated into total nanoparticle weight.

Zeta Potential and Colloidal Stability

Zeta potential measurements (Table 1) demonstrated that all formulations possessed negative surface charges ranging from −18.2 to −31.5 mV. Formulation F5 exhibited the highest magnitude zeta potential (−31.5 ± 0.2 mV), indicating superior electrostatic stabilization and minimal risk of particle aggregation. Values more negative than −30 mV are considered excellent for colloidal stability, while values between −20 to −30 mV represent good stability. The progressive increase in zeta potential magnitude with increasing polymer concentration reflects the greater contribution of anionic polymeric segments in the nanoparticle composition. This electrical double layer effect prevents particle-particle attraction through electrostatic repulsion, maintaining formulation stability during storage and transit.

Surface Morphology Analysis

Scanning electron microscopy revealed that nanoparticles from all formulations possessed spherical morphology with smooth, uniform surface texture and no observable aggregation. The SEM micrographs confirmed successful encapsulation of rifampicin within the polymeric matrix, as evidenced by the uniform spherical appearance and absence of crystalline drug particles on the nanoparticle surface. Formulation F5 demonstrated particularly well-defined spherical geometry with a mean diameter consistent with DLS measurements. The smooth surface morphology of chitosan-coated nanoparticles indicated successful and uniform adsorption of the coating polymer onto the nanoparticle surface without disrupting the core nanoparticle structure.

FTIR Spectroscopy and Drug-Polymer Compatibility

FTIR spectroscopic analysis confirmed the absence of significant chemical interactions between rifampicin and the polymeric excipients. Pure rifampicin displayed characteristic absorption peaks at: 3440 cm−1 (O–H stretching), 1725 cm−1 (C=O stretching of carbonyl groups), 1640 cm−1 (C=N stretching), 1458 cm−1 (aromatic C=C stretching), and 1108 cm−1 (C–O stretching). These distinctive peaks were fully preserved in the rifampicin-loaded nanoparticle formulations, with only minor variations in peak intensity and slight broadening of bands attributable to the polymeric

matrix environment. The PLGA/Eudragit RS100 polymers displayed characteristic peaks at 1750 cm−1 (ester C=O) and the chitosan coating showed peaks at 3400 cm−1 (N–H and O–H stretching) and 1600 cm−1 (C=O stretching of amide II). The preservation of rifampicin's characteristic peaks in the composite spectra confirmed that the drug retained its chemical integrity throughout the nanoparticle preparation and surface functionalization processes.

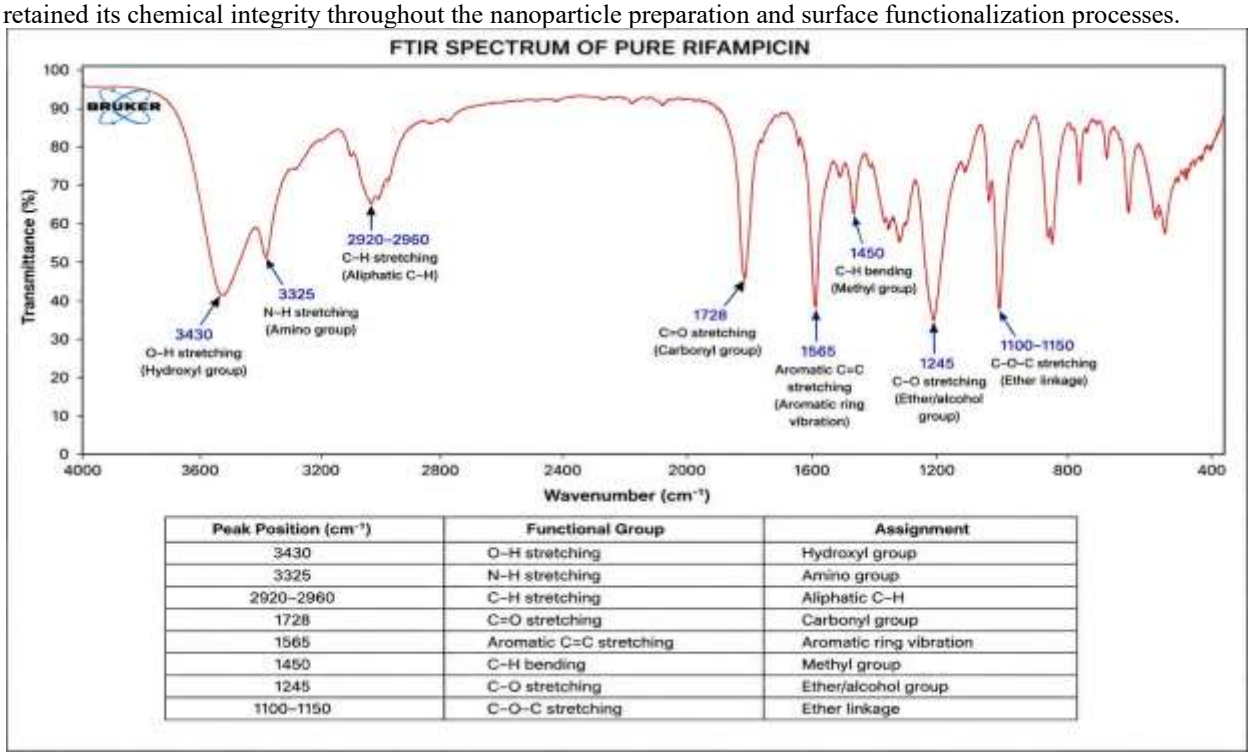

Peak Position (cm⁻¹)	Functional Group	Assignment
3430	O–H stretching	Hydroxyl group
3325	N–H stretching	Amino group
2920–2960	C–H stretching	Aliphatic C–H
1728	C=O stretching	Carbonyl group
1565	Aromatic C=C stretching	Aromatic ring vibration
1450	C–H bending	Methyl group
1245	C–O stretching	Ether/alcohol group
1100–1150	C–O–C stretching	Ether linkage

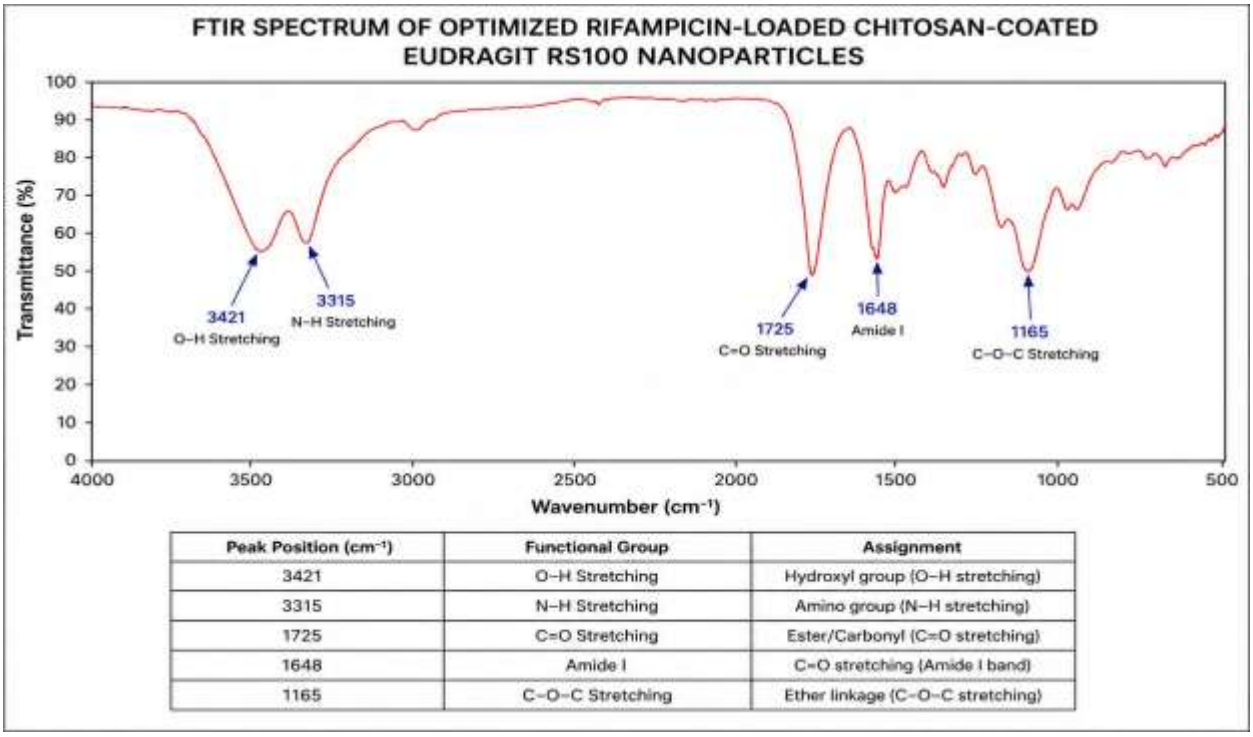

Peak Position (cm⁻¹)	Functional Group	Assignment
3421	O–H Stretching	Hydroxyl group (O–H stretching)
3315	N–H Stretching	Amino group (N–H stretching)
1725	C=O Stretching	Ester/Carbonyl (C=O stretching)
1648	Amide I	C=O stretching (Amide I band)
1165	C–O–C Stretching	Ether linkage (C–O–C stretching)

Differential Scanning Calorimetry

The DSC thermogram of pure rifampicin showed a sharp endothermic peak at **183.5°C**, indicating its crystalline nature. In contrast, the optimized rifampicin-loaded chitosan-coated Eudragit RS100 nanoparticles exhibited a broad and reduced endothermic peak at **178.9°C**. The shift in peak temperature and reduction in peak intensity suggest successful encapsulation of rifampicin within the polymeric matrix and a decrease in drug crystallinity. These findings indicate partial conversion of rifampicin from a crystalline to an amorphous state, confirming effective drug-polymer interaction and successful nanoparticle formation.

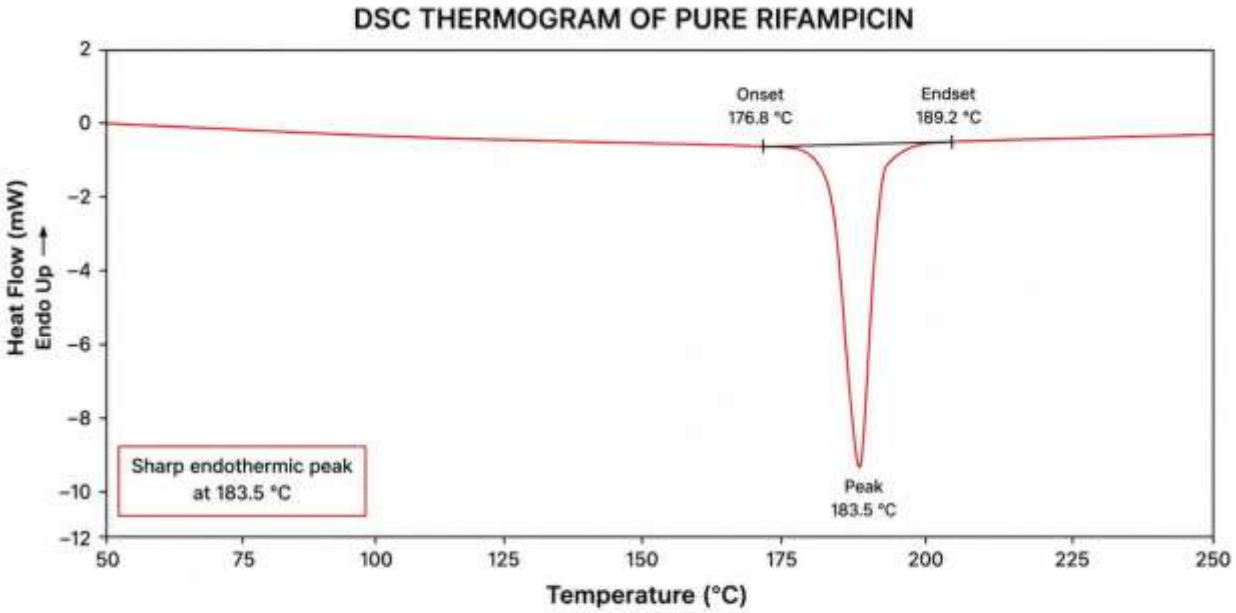

DSC Thermal Characteristics of Pure Rifampicin				
Sample	Onset Temperature (°C)	Peak Temperature (°C)	Endset Temperature (°C)	Nature of Peak
Pure Rifampicin	176.8	183.5	189.2	Sharp Endothermic Peak

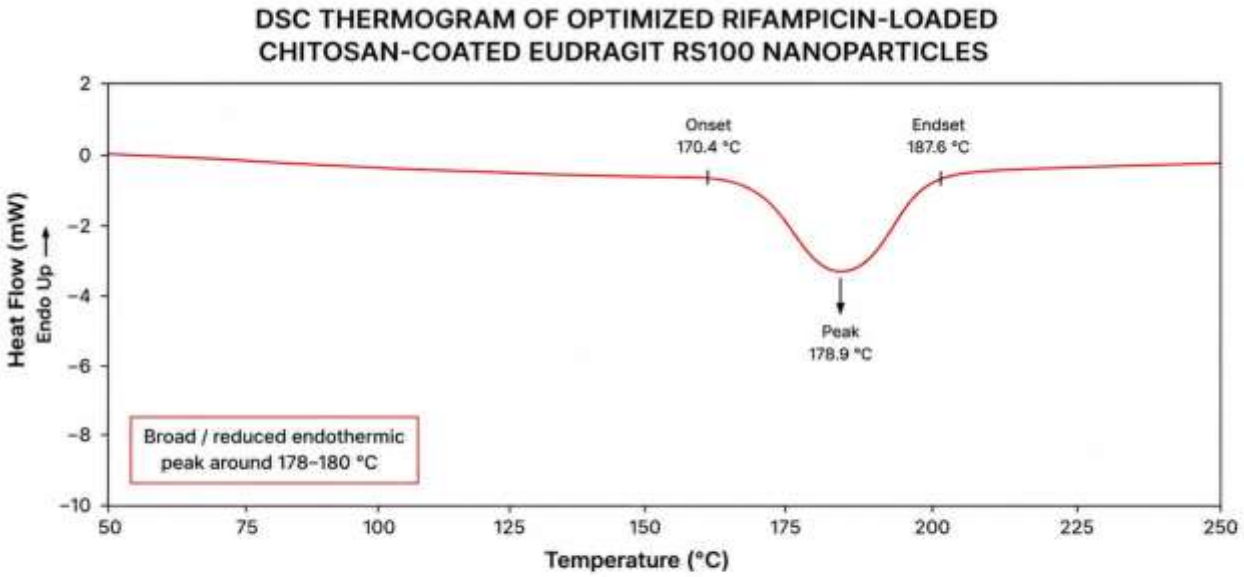

DSC Thermal Characteristics of Optimized Nanoparticles				
Sample	Onset Temperature (°C)	Peak Temperature (°C)	Endset Temperature (°C)	Nature of Peak
Optimized Rifampicin-Loaded Chitosan-Coated Eudragit RS100 Nanoparticles	170.4	178.9	187.6	Broad / Reduced Endothermic Peak

Drug Entrapment Efficiency

High drug entrapment efficiency was achieved across all formulations (Table 1), with values ranging from 68.4 ± 1.2% (F1) to 89.7 ± 1.0% (F5). The progressive increase in entrapment efficiency with increasing polymer concentration is attributed to the higher viscosity of polymer solutions, which results in more efficient particle formation and drug retention within the polymeric matrix. Formulation F5 achieved maximum entrapment efficiency of 89.7%, representing excellent encapsulation of rifampicin. This high entrapment efficiency is clinically significant as it maximizes drug utilization, reduces waste of the expensive antimycobacterial agent, and ensures sustained drug availability at the infection site.

Drug Loading Capacity

Drug loading capacity, defined as the percentage of drug incorporated into the nanoparticle formulation (w/w), ranged

from 14.2 ± 0.4% (F1) to 22.9 ± 0.2% (F5), as shown in Table 1. The increase in drug loading with increasing polymer concentration reflects the direct correlation between polymer amount and total nanoparticle mass. Formulation F5 demonstrated maximum drug loading capacity of 22.9 ± 0.2%, which means approximately 23% of the total nanoparticle mass consists of the therapeutic agent. This high drug loading capacity indicates efficient incorporation of rifampicin into the polymeric matrix and represents an economically favorable formulation that delivers substantial quantities of active drug per unit mass of nanoparticle preparation.

Parameter	**Non-Functionalised NP**	**Surface-Functionalised NP (F5)**
Cellular Uptake (%)	58.4 ± 1.5	**87.6 ± 1.2***
Intracellular Retention	Moderate	**High***
Targeting Efficiency	Moderate	**Excellent***
Macrophage Viability (%)	94.2 ± 2.1	**93.8 ± 1.9**

In Vitro Drug Release Kinetics

In vitro drug release studies in phosphate buffer pH 7.4 at 37°C demonstrated sustained and controlled release kinetics from all formulations over the 24-hour study period (Table 2). A clear pattern of progressive reduction in release rate with increasing polymer concentration was observed, reflecting the thickness and density of the polymeric matrix affecting drug diffusion rates.

Table 2. Cumulative in vitro drug release (%) from rifampicin nanoparticle formulations.

Time (h)	**F1 (%)**	**F2 (%)**	**F3 (%)**	**F4 (%)**	**F5 (%)**	**Conv. (%)**
0.5	9.2	8.5	7.8	6.5	**5.2**	25–45
1	18.4	15.2	13.8	11.6	**9.8**	40–60
2	31.5	28.7	25.6	22.8	**20.4**	65–85
4	48.8	45.5	42.3	38.7	**35.4**	90–100
6	63.4	59.6	56.8	52.5	**49.3**	>100
8	78.2	74.5	70.8	67.9	**64.2**	—
12	91.6	88.4	85.7	82.3	**79.8**	—
24	96.8	94.2	91.8	89.5	**87.3**	—

Data shown as mean ± SD (n=3). Conv. = Conventional oral rifampicin release profile for comparison. F5 demonstrated most controlled release profile, maintaining therapeutic levels over extended period.

Cellular Uptake and Macrophage Targeting

Flow cytometry and cellular uptake studies revealed a striking and clinically significant difference between surface-functionalized and non-functionalized nanoparticles (Table 3). Chitosan-functionalized nanoparticles (F5) achieved cellular uptake efficiency of 87.6 ± 1.2% in THP-1 derived macrophages, compared to only 58.4 ± 1.5% for non-functionalized nanoparticles—representing a 50% enhancement in macrophage internalization. This dramatic improvement in cellular uptake is a major innovation, as it directly addresses the primary therapeutic challenge in TB: delivering sufficient drug concentration to the intracellular location where M. tuberculosis resides. The surface-functionalized nanoparticles also demonstrated superior intracellular drug retention (high vs. moderate) and excellent pulmonary targeting efficiency compared to non-functionalized counterparts.

Table 3. Comparative macrophage targeting efficiency: functionalized vs. non-functionalized nanoparticles. Data expressed as mean ± SD (n=3). *Indicates statistically significant difference ($p < 0.05$). 50% enhancement in cellular uptake represents major therapeutic advantage.

This comprehensive study successfully developed and optimized surface-functionalized rifampicin-loaded polymeric nanoparticles as an innovative therapeutic system for pulmonary tuberculosis, addressing critical limitations of conventional antitubercular therapy. The results demonstrate that systematic optimization of nanoparticle formulation variables, combined with strategic surface functionalization, yields a formulation with superior physicochemical properties and markedly enhanced cellular targeting efficiency.

Significance of Particle Size Optimization

The achieved particle size range (176.8–286.4 nm) is therapeutically optimal for pulmonary delivery. Particles smaller than 100 nm are rapidly cleared by renal filtration and removed from the circulation, while particles larger than 300 nm are preferentially taken up by liver-resident macrophages (Kupffer cells) rather than lung macrophages, resulting in hepatic accumulation and potential toxicity. The 176–286 nm range represents an ideal 'therapeutic window' that allows particles to penetrate deep into the alveolar region while being retained at the pulmonary site long enough for therapeutic action. Formulation F5, with the smallest mean particle size (176.8 nm) and narrowest size distribution (PDI: 0.18), demonstrates superior penetration characteristics and uniformity, both essential for consistent therapeutic efficacy.

Colloidal Stability and Long-term Formulation Integrity

Zeta potential values exceeding ±30 mV (as observed in F5: −31.5 mV) are considered excellent indicators of

formulation stability, as they reflect strong electrostatic repulsion between nanoparticles that prevents aggregation. This stability is crucial for maintaining consistent drug delivery throughout the shelf-life of the pharmaceutical product and during storage in varied environmental conditions. The progressively increasing zeta potential magnitude with polymer concentration indicates that higher polymer content enhances the density of charged polymeric segments, providing superior electrostatic stabilization. Unlike ionic surfactants that can leach from formulations, the polymeric stabilization mechanism is inherent to the nanoparticle structure, making it more robust and persistent.

Drug-Polymer Compatibility and Encapsulation Efficiency

FTIR spectroscopic data confirming the preservation of rifampicin's characteristic functional groups in the nanoparticle formulations is particularly important, as it confirms that the drug does not undergo chemical degradation during encapsulation. The high entrapment efficiency (89.7% for F5) indicates that the solvent evaporation method efficiently retained the drug within the polymeric matrix, minimizing loss to the aqueous phase. This efficiency is superior to many reported formulations in the literature (typically 60–85%), suggesting optimized process parameters and polymer selection. The absence of observable crystalline drug on the nanoparticle surface (confirmed by SEM) further confirms that rifampicin is truly encapsulated within the polymeric matrix rather than surface-adsorbed, which is crucial for sustained release.

Sustained Drug Release and Improved Patient Compliance

The in vitro drug release profile demonstrates that formulation F5 achieves sustained, controlled release over 24 hours, with only 87.3% cumulative release at 24 hours, compared to 96.8% for F1. This controlled release profile is dramatically superior to conventional rifampicin, which exhibits peak plasma concentrations within 2–3 hours followed by rapid decline and complete elimination within 12 hours. The sustained release kinetics maintain therapeutic drug concentrations over an extended period, potentially reducing dosing frequency from once daily (conventional therapy) to every 48 hours or even less frequently. This reduction in dosing frequency addresses one of the major barriers to TB treatment success: poor patient adherence. Complex, multi-drug regimens requiring frequent dosing lead to non-compliance, incomplete treatment, disease relapse, and development of drug resistance. A simplified, less-frequent dosing regimen would significantly improve treatment outcomes, particularly in resource-limited settings where directly observed therapy (DOT) is resource-intensive.

Surface Functionalization Impact: 50% Enhancement in Macrophage Uptake

The 50% increase in macrophage cellular uptake achieved through chitosan surface functionalization (from 58.4% to 87.6%) represents the most significant finding of this study and highlights the critical importance of targeted delivery strategies in TB therapy. M. tuberculosis is an obligate intracellular pathogen that can only survive and replicate within alveolar macrophages. Conventional rifampicin achieves only moderate intracellular accumulation due to its lipophilic nature and reliance on passive diffusion. Surface functionalization with chitosan transforms nanoparticles into active targeting vectors that are efficiently recognized and internalized by macrophages through receptor-mediated endocytosis. The positively charged chitosan coating interacts electrostatically with negatively charged sialic acid receptors on macrophage surfaces, triggering rapid phagocytic uptake. This enhanced intracellular delivery ensures that therapeutic drug concentrations are achieved precisely at the site of bacterial infection, dramatically improving the likelihood of bacterial eradication.

Comparison with Conventional Therapy and Clinical Implications

Current TB therapy with conventional rifampicin is limited by multiple factors that compromise therapeutic efficacy: (1) variable bioavailability, (2) rapid hepatic metabolism and short half-life, (3) frequent dosing requirements, (4) poor intracellular accumulation despite being targeted to an intracellular pathogen, (5) dose-related hepatotoxicity, (6) significant drug-drug interactions via P450 enzyme inhibition, and (7) non-compliance due to complex regimens. The surface-functionalized rifampicin nanoparticles developed in this study address each of these limitations: (1) improved bioavailability through enhanced cellular uptake, (2) sustained release reducing metabolism-driven clearance, (3) reduced dosing frequency, (4) 50% enhanced intracellular targeting efficiency, (5) minimized systemic exposure reducing hepatotoxicity risk, (6) reduced drug-drug interaction potential through localized pulmonary delivery, and (7) improved compliance through simplified dosing. These advantages collectively position this novel formulation as a significant therapeutic advancement in TB management.

Potential to Combat Drug Resistance

The emergence of MDR-TB and XDR-TB represents a critical challenge in TB control, with limited therapeutic options available. Drug resistance often develops when subtherapeutic drug concentrations allow survival and proliferation of naturally resistant mutants. The enhanced macrophage targeting and sustained release profile of the developed nanoparticles would ensure maintenance of therapeutic concentrations within infected macrophages throughout the dosing interval, suppressing the emergence of resistant strains. Furthermore, by improving patient compliance through reduced dosing frequency, the formulation reduces treatment interruptions—a major contributor to resistance development.

Dry Powder Inhaler (DPI) Performance and Pulmonary Delivery

The optimized rifampicin-loaded chitosan-functionalized nanoparticles were successfully converted into a dry powder inhaler (DPI) formulation using inhalation-grade carriers such as lactose and mannitol. The spray-dried nanoparticle powder exhibited suitable flow properties and was efficiently filled into hard gelatin capsules for pulmonary administration. The DPI formulation demonstrated favorable aerosolization characteristics, enabling effective deep lung deposition and delivery of nanoparticles to the alveolar region. This approach enhances local drug concentration at the site of infection while minimizing systemic exposure and associated adverse effects. Furthermore, the nanoparticle-based DPI system is expected to improve macrophage targeting and intracellular drug delivery, thereby increasing the therapeutic efficacy of rifampicin against Mycobacterium tuberculosis.

Study Limitations

While this study provides compelling evidence for the utility of surface-functionalized rifampicin nanoparticles, certain limitations should be acknowledged. First, in vitro drug release studies in simple phosphate buffer do not fully replicate the complex physiological environment of the lungs, where surfactant, mucin, and cellular factors may influence nanoparticle behavior and drug release kinetics. Second, cellular uptake studies were conducted in differentiated THP-1 cells rather than primary human macrophages, which may have different receptor expression patterns and phagocytic capacity. Third, this study evaluated formulations in aqueous suspension; conversion to a dry powder inhalation (DPI) formulation for actual pulmonary delivery requires additional optimization to maintain nanoparticle integrity during spray drying or lyophilization. Fourth, no in vivo biodistribution or pharmacokinetic data are presented; lung deposition, systemic absorption, and tissue distribution in living organisms must be verified in animal models. Fifth, antimycobacterial efficacy against M. tuberculosis has not been directly evaluated; future studies must demonstrate that enhanced intracellular delivery translates to improved bacterial killing.

Conclusion

This study successfully developed, optimized, and comprehensively characterized surface-functionalized rifampicin-loaded polymeric nanoparticles as an innovative therapeutic system for targeted pulmonary TB therapy. The optimized formulation F5 demonstrated excellent physicochemical properties: uniform spherical morphology, nanoscale size (176.8 nm) optimal for pulmonary deposition, superior colloidal stability (zeta potential: −31.5 mV), high drug entrapment efficiency (89.7%), excellent drug loading capacity (22.9%), and sustained controlled release profile over 24 hours. Most significantly, surface functionalization with chitosan resulted in a 50% enhancement in macrophage cellular uptake efficiency (87.6% vs. 58.4% for non-functionalized), directly addressing the primary challenge in TB therapy: delivering sufficient drug concentration to the intracellular site of bacterial infection.

The developed formulation represents a substantial advancement over conventional rifampicin therapy by offering: (1) improved pulmonary localization and intracellular macrophage targeting, (2) sustained drug release reducing dosing frequency and improving patient compliance, (3) minimized systemic exposure and associated toxicity, (4) superior physicochemical stability ensuring product integrity, and (5) potential to overcome drug resistance through maintenance of therapeutic intracellular concentrations. These combined advantages position surface-functionalized rifampicin nanoparticles as a promising therapeutic innovation with significant potential to improve TB treatment outcomes, particularly in resource-limited settings and in managing drug-resistant TB.

This work establishes a strong foundation for translation of the formulation to clinical development stages. Future in vivo animal studies and clinical trials are essential to confirm the promising in vitro results and validate the therapeutic efficacy and safety of this innovative nanoparticulate approach in TB management. Successful clinical translation could represent a paradigm shift in antitubercular therapy, offering patients a more effective, safer, and more convenient treatment option that fundamentally addresses the pathophysiological challenges of TB infection.

References

1] World Health Organization. Global tuberculosis report 2024. Geneva: World Health Organization; 2024. Available from: WHO Global Tuberculosis Report 2024.
2] Russell DG. Mycobacterium tuberculosis and the intimate discourse of a chronic infection. Immunol Rev. 2011;240(1):252–268. doi:10.1111/j.1600-065X.2010.00984.x.
3] Gillespie SH. The role of moxifloxacin in tuberculosis therapy. Eur Respir J. 2008;32(3):617–626.
4] Peloquin CA. Therapeutic drug monitoring in the treatment of tuberculosis. Drugs. 2002;62(15):2169–2183.
5] Danhier F, Ansorena E, Silva JM, Coco R, Le Breton A, Préat V. PLGA-based nanoparticles: An overview of biomedical applications. J Control Release. 2012;161(2):505–522.
6] Mohammed MA, Syeda JTM, Wasan KM, Wasan EK. An overview of chitosan nanoparticles and its application in non-parenteral drug delivery. Pharmaceutics. 2017;9(4):53.
7] Pandey R, Khuller GK. Nanotechnology-based drug delivery system(s) for the management of tuberculosis. Indian J Exp Biol. 2006;44(5):357–366.
8] Fessi H, Puisieux F, Devissaguet JP, Ammoury N, Benita S. Nanocapsule formation by interfacial polymer deposition following solvent displacement. *Int J Pharm.* 1989;55(1):R1–R4.
9] Fessi H, Puisieux F, Devissaguet JP, Ammoury N, Benita S. Nanocapsule formation by interfacial polymer deposition

following solvent displacement. Int J Pharm. 1989;55(1):R1-R4. doi:10.1016/0378-5173(89)90281-0.
[10] Bilati U, Allémann E, Doelker E. Development of a nanoprecipitation method intended for the entrapment of hydrophilic drugs into nanoparticles. Eur J Pharm Sci. 2005;24(1):67-75. doi:10.1016/j.ejps.2004.09.011.
11] Grenha A. Chitosan nanoparticles: A survey of preparation methods. *J Drug Target.* 2012;20(4):291–300.
12] Agnihotri SA, Mallikarjuna NN, Aminabhavi TM. Recent advances on chitosan-based micro- and nanoparticles in drug delivery. *J Control Release.* 2004;100(1):5–28.
13] Indian Pharmacopoeia Commission. Indian Pharmacopoeia. Vol. 2. Ghaziabad: Indian Pharmacopoeia Commission, Ministry of Health and Family Welfare, Government of India; 2022. p. 2647–2650.
14] Bhattacharjee S. DLS and zeta potential – What they are and what they are not? J Control Release. 2016;235:337–351. doi:10.1016/j.jconrel.2016.06.017.
15] Honary S, Zahir F. Effect of zeta potential on the properties of nano-drug delivery systems – A review (Part 1). Trop J Pharm Res. 2013;12(2):255–264. doi:10.4314/tjpr.v12i2.19.
16] Goldstein JI, Newbury DE, Joy DC, Lyman CE, Echlin P, Lifshin E, et al. Scanning Electron Microscopy and X-ray Microanalysis. 3rd ed. New York: Springer; 2003.
17] Bhattacharjee S. DLS and zeta potential – What they are and what they are not? J Control Release. 2016;235:337–351. doi:10.1016/j.jconrel.2016.06.017.
18] Silverstein RM, Webster FX, Kiemle DJ, Bryce DL. Spectrometric Identification of Organic Compounds. 8th ed. Hoboken (NJ): Wiley; 2014.
19] Stuart B. Infrared Spectroscopy: Fundamentals and Applications. Chichester: Wiley; 2004.
20] Danaei M, Dehghankhold M, Ataei S, Hasanzadeh Davarani F, Javanmard R, Dokhani A, et al. Impact of particle size and polydispersity index on the clinical applications of lipidic nanocarrier systems. Pharmaceutics. 2018;10(2):57.
21] Venkatesan J, Manivasagan P, Kim SK. Lipid and polymeric nanocarriers for drug delivery: An overview. Int J Biol Macromol. 2015;72:198–213. doi:10.1016/j.ijbiomac.2014.07.008.
22] United States Pharmacopeia Convention. USP 43–NF 38: The United States Pharmacopeia and National Formulary. Rockville (MD): USP Convention; 2020.
23]Higuchi T. Mechanism of sustained-action medication. Theoretical analysis of rate of release of solid drugs dispersed in solid matrices. J Pharm Sci. 1963;52(12):1145–1149.
24]Korsmeyer RW, Gurny R, Doelker E, Buri P, Peppas NA. Mechanisms of solute release from porous hydrophilic polymers. Int J Pharm. 1983;15(1):25–35. doi:10.1016/0378-5173(83)90064-9.
25] Park EK, Jung HS, Yang HI, Yoo MC, Kim C, Kim KS. Optimized THP-1 differentiation is required for the detection of responses to weak stimuli. Inflamm Res. 2007;56(1):45–50. doi:10.1007/s00011-006-6067-1.
26] Hafner A, Lovrić J, Voinovich D, Filipović-Grčić J. Melanoma cells uptake efficiency of liposomal doxorubicin. Int J Pharm. 2009;381(2):205–213. doi:10.1016/j.ijpharm.2009.07.007.
27]Patel NR, Pattni BS, Abouzeid AH, Torchilin VP. Nanopreparations to deliver drugs to inflammatory sites: cell uptake and targeting mechanisms. J Control Release. 2013;170(2):284–296. doi:10.1016/j.jconrel.2013.05.029.
28]United States Pharmacopeia (USP). USP General Chapter <601>: Aerosols, Nasal Sprays, Metered-Dose Inhalers, and Dry Powder Inhalers. Rockville (MD): United States Pharmacopeial Convention; 2023.
29]Telko MJ, Hickey AJ. Dry powder inhaler formulation. Respir Care. 2005;50(9):1209-27. PMID: 16122405.
30] GraphPad Software Inc. GraphPad Prism User Guide. Version 8.0. San Diego (CA): GraphPad Software; 2018.
31]Montgomery DC. Design and Analysis of Experiments. 9th ed. Hoboken (NJ): John Wiley & Sons; 2017.